HYDROLOGICAL PROCESSES
Hydrol. Process. **24**, 3603–3620 (2010)
Published online 20 July 2010 in Wiley Online Library
(wileyonlinelibrary.com) DOI: 10.1002/hyp.7786

Snowmelt energetics at a shrub tundra site in the western Canadian Arctic

P. Marsh,[1]* P. Bartlett,[2] M. MacKay,[2] S. Pohl[3] and T. Lantz[4]

[1] *National Hydrology Research Centre, Environment Canada, Saskatoon, SK, Canada*
[2] *Climate Research Division, Environment Canada, Toronto, ON, Canada*
[3] *Centre for Hydrology, University of Saskatchewan, Saskatoon, SK, Canada*
[4] *School of Environmental Studies, University of Victoria, Victoria, BC, Canada*

Abstract:

Snow accumulation and melt were observed at shrub tundra and tundra sites in the western Canadian Arctic. End of winter snow water equivalent (SWE) was higher at the shrub tundra site than the tundra site, but lower than total winter snowfall because snow was removed by blowing snow, and a component was also lost to sublimation. Removal of snow from the shrub site was larger than expected because the shrubs were bent over and covered by snow during much of the winter. Although SWE was higher at the shrub site, the snow disappeared at a similar time at both sites, suggesting enhanced melt at the shrub site. The Canadian Land Surface Scheme (CLASS) was used to explore the processes controlling this enhanced melt. The spring-up of the shrubs during melt had a large effect on snowmelt energetics, with similar turbulent fluxes and radiation above the canopy at both sites before shrub emergence and after the snowmelt. However, when the shrubs were emerging, conditions were considerably different at the two sites. Above the shrub canopy, outgoing shortwave radiation was reduced, outgoing longwave radiation was increased, sensible heat flux was increased and latent flux was similar to that at the tundra site. Above the snow surface at this site, incoming shortwave radiation was reduced, incoming longwave radiation was increased and sensible heat flux was decreased. These differences were caused by the lower albedo of the shrubs, shading of the snow, increased longwave emission by the shrub stems and decreased wind speed below the shrub canopy. The overall result was increased snowmelt at the shrub site. Although this article details the impact of shrubs on snow accumulation and melt, and energy exchanges, additional research is required to consider the effect of shrub proliferation on both regional hydrology and climate.

KEY WORDS shrub tundra; surface energetics; snowmelt; climate change; hydrology

Received 7 October 2009; Accepted 10 May 2010

INTRODUCTION

Air temperatures have been rising in both Alaska (Sturm *et al*., 2001a; ACIA, 2005) and the western Canadian Arctic (Marsh *et al*., 2002; ACIA, 2005; Lantz and Kokelj, 2008; Burn and Kokelj, 2009) over the last few decades, and global climate models (GCMs) suggest that the Arctic will continue to warm more rapidly than more southerly locations (ACIA, 2005). The portion of the Arctic biome that is predicted to respond most rapidly to this warming is the transition between upright and dwarf shrub tundra (Epstein *et al*., 2004). This prediction has been corroborated by experimental manipulations of temperature resulting in increases in the height and cover of deciduous shrubs, evidence of increasing shrub cover on air photos, observational studies of shrub population structure across regional temperature gradients and the changes to vegetation indices derived from satellites (Chapin *et al*., 1995; Sturm *et al*., 2001b; Goetz, 2005; Tape *et al*., 2006; Walker *et al*., 2006; Olthof *et al*., 2008; Lantz *et al*., 2010a,b).

* Correspondence to: P. Marsh, National Hydrology Research Centre, Environment Canada, Saskatoon, SK, Canada.
E-mail: philip.marsh@ec.gc.ca

Shrub proliferation is anticipated to affect snowpack depth, snow water equivalent (SWE), melt rate and duration of the snow-covered period, but there is uncertainty about the magnitude and direction of these changes. Sturm *et al*. (2001a) and Liston (2002) outlined the potential effects of shrubs on snow accumulation and suggested that an increase in the abundance of shrubs would result in increased snow depth and SWE due to fewer occurrences of blowing snow and therefore reduced sublimation over the winter period. Other studies (Essery and Pomeroy, 2004; Bewley, 2006; Pomeroy *et al*., 2006; Lantz *et al*., 2009) have shown that snow accumulation in areas with shrubs is dependent on shrub density and height, with taller shrubs typically retaining more snow. Shrubs affect the melt of this deeper snowpack by reducing the albedo (Sturm *et al*., 2005), shading the snowpack (Bewley, 2006), re-radiating longwave radiation from warm shrub branches (Bewley, 2006; Pomeroy *et al*., 2006) and reducing turbulent fluxes of sensible and latent heat due to reduced wind speed (Bewley, 2006). The effect of shrubs on each energy balance component controlling the melt rate is dependent on shrub density and spacing (Bewley, 2006), with the overall effect of shrubs to accelerate melt (Endrizzi and Marsh, 2009).

Marsh *et al.* (2003), Sturm *et al.* (2005) and Pomeroy *et al.* (2006) have shown that the role of shrubs on both snow accumulation and melt is further complicated by the fact that under certain conditions shrubs may be bent over and buried by snow during the winter. Although the shrubs bent over and buried by snow, shrub surfaces behave like tundra surfaces during both the snow accumulation period and the snowmelt period. After sufficient melt, the shrubs emerge from the snowpack, exerting a strong impact on the radiation balance and wind speed at the surface, therefore, on melt rates.

Although a large portion of the low Arctic is likely to be influenced by shrub encroachment (Epstein *et al.*, 2004; Tape *et al.*, 2006), variation in snow–shrub interactions with shrub density suggests that the impact of shrub expansion on snow accumulation and melt may vary across regional and global scales. One of the few studies to consider the impact of shrubs on regional climate was Strack *et al.* (2007), who used regional climate simulations to suggest that a complete change from tundra to shrub tundra in northern Alaska would result in earlier melt and warmer air temperatures. However, there are still considerable uncertainties in our understanding of both the role of shrubs on snow accumulation and melt, and our ability to accurately describe the hydrology and surface–atmosphere exchanges of shrub areas using current land surface or hydrologic models. As a result, our ability to predict the impact of increasing shrub area and density on future hydrology, and on the regional climate, is not well known. In order to address these issues, this study examines the role of shrubs on snow accumulation and melt, and utilizes the CLASS (Verseghy, 1991) to explore the processes controlling energy exchange and snowmelt for tundra and shrub tundra surfaces. Future research will upscale the results from this case study to examine the role of variation in tall tundra, dwarf shrub and forest cover at the landscape scale.

STUDY AREA AND METHODS

Location

Field observations were obtained in the vicinity of the Trail Valley Creek (TVC) research basin (68°45′N, 133°30′W) (Figure 1) located immediately east of the Mackenzie Delta and approximately 55 km north east of Inuvik, Northwest Territories (NWT) during April to June 2003, when research personal were on site at the end of winter and during the snowmelt period. To supplement this record, end of winter snow surveys and instrument observations were obtained for the period 2004–2007. This article focuses on the most intensive period of observation in 2003, but to consider key aspects of inter-annual variability, we also utilize data from the other study years. The TVC research basin is approximately 57 km^2 in area (Marsh *et al.*, 2007), and is characterized by gently rolling hills with some deeply incised river valleys, and elevations that range from 9 to 187 m.a.s.l., with an average elevation of 99 m.a.s.l. The region is located in the continuous permafrost zone (Heginbottom and Dubreuil, 1995), and lies at the northern edge of the forest–tundra transition zone with a mix of dwarf shrub and herbaceous tundra (referred to throughout as tundra), and upright shrub tundra (shrub), and woodlands (Corns, 1974; Burn and Kokelj, 2009) (Figure 1). Examples of shrub expansion have been noted in the region (MacKay, 1995, 1998, 1999; Lantz *et al.*, 2010b), but the area affected and the rate of change have not been documented in detail. However, Goetz *et al.* (2005) used satellite Normalized Difference Vegetation Index (NDVI) data to show that for the Mackenzie Delta region of NW Canada, the trend in photosynthetic activity was either positive or strongly positive, suggesting an increase in shrub density and areal extent.

Detailed studies of the redistribution of snow in the TVC basin due to frequent blowing snow events (Pomeroy *et al.*, 1997, 2007; Essery *et al.*, 1999) have shown that tundra areas within the basin act as a source of blowing snow, while the edges of areas with taller shrub and forest vegetation become sinks. Lake margins, stream channels and slopes with gradients exceeding 9° are also sinks for blowing snow. As a result, the spatial variation of SWE is large, as indicated by the winter of 1993, a typical year, when SWE varied from 54 to 419% of measured snow fall at the end of winter (Pomeroy *et al.*, 1997). In addition to variability in SWE amongst landcover types, Pomeroy *et al.* (1998) and Essery *et al.* (1999) point out that there is also considerable variation within each landcover class. They showed that exposed parts of the basin had higher coefficients of variation (CV = 0·42 for open tundra), while sheltered and more densely vegetated areas tended to have lower CVs (CV = 0·11 for sparsely forested regions). Pohl and Marsh (2006) used this information to estimate the spatial variability in the end of winter SWE at TVC.

Snowmelt in the region usually occurs during May and June (Marsh *et al.*, 2002). Using air temperature as a proxy for estimating the melt period, Marsh *et al.* (2002) showed that on average, mid-day air temperatures first rise above 0 °C at the Inuvik airport on April 28, and remain above 0 °C after May 17. However, there is large variability, with the earliest above 0 °C temperature occurring on April 9, and the date of continuous mid-day temperatures above 0 °C varying from April 23 to May 29.

Observations

Meteorological stations operated in the TVC area include: the TVC upper plateau (TUP) station located in an area of tundra vegetation; the TVC main meteorological (TMM) station in an area of mixed low shrub tundra and tundra and the TVC tall shrub (TTS) station located just outside the TVC basin, within an area of tall shrubs (Figures 1 and 2). This study focuses on snow accumulation and melt above shrub (TTS) and tundra (TUP) surfaces. Where appropriate we also employ data from TMM.

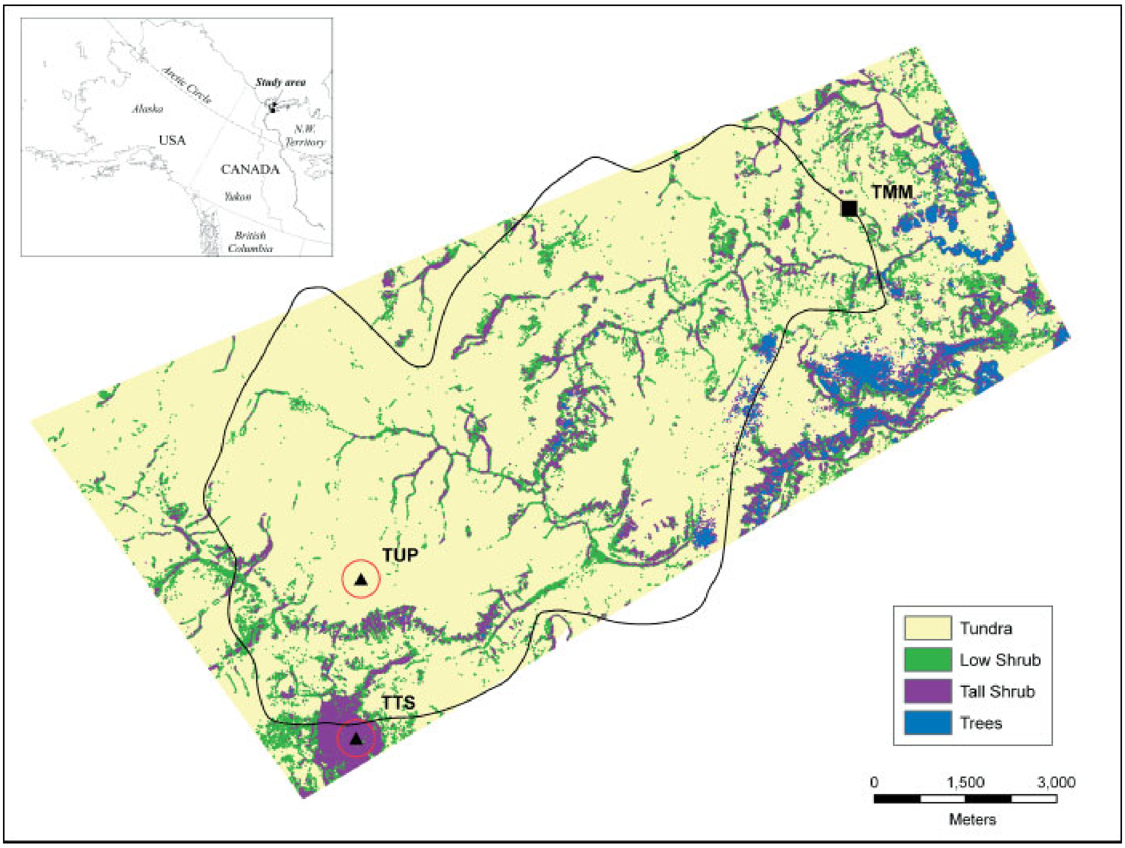

Figure 1. Trail Valley Creek (with basin boundary shown by black line, with the basin outlet to the east) vegetation height classes derived from LiDAR, with tundra defined as areas with vegetation <0·50 m, low shrub defined as vegetation >0·50 and <1·25 m, tall shrubs >1·25 and <3·0 m, and trees >3·0 m in height. The tundra (TUP) and shrub tundra (TTS) meteorological stations are marked by black triangles with a 300 m diameter circle around them. The main meteorological (TMM) station is in a tundra/shrub area marked by a square

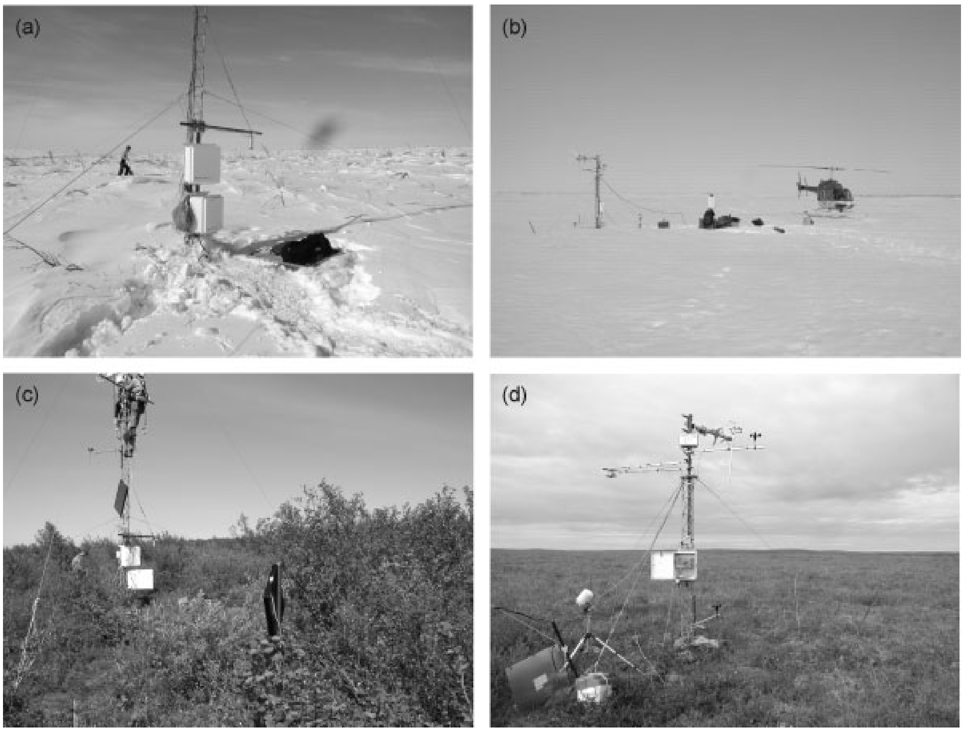

Figure 2. Micrometeorological towers for the shrub site (a) and tundra site (b) at the end of winter and during summer (c and d). Note that at the end of winter, the alder shrubs are bent over and mostly covered by the shallow snow cover in mid-April 2003 (a)

The TTS site is characterized by a large expanse of continuous tall shrub cover that is unique in the TVC area (Figure 1). However, it is similar to areas of extensive shrub cover located approximately 15–20 km to the south (MacKay, 1995). Fetch for the TTS site is 560 m to the north and west, 330 m to the east, and 2000 m to the south, while fetch at TUP is greater than 600 m in all directions. Due to the size of the TTS site, edge effects are small and this site likely has snow accumulation and melt characteristics similar to a continuous expanse of shrub.

A full suite of meteorological measurements were made at TUP, TTS and TMM (Table I). At TTS, measurements were obtained both well above the canopy and near the surface. These near-surface measurements were typically below the top of the canopy; however, when the shrubs are bent over and buried in snow they were made above the canopy (Figure 2a). In addition (as discussed below), the shrubs at this site do not comprise a closed canopy even when fully emerged (Figure 2c), and as a result the measurements below the top of the shrubs often have a nearly unobstructed view of the sky. At TUP, the late winter snow completely covered the low tundra vegetation (2b) and the instruments are always above the canopy (2d).

Measurements of turbulent fluxes of sensible and latent heat were obtained at both TUP and TTS by the eddy covariance method using common instrumentation (Table I). Fluxes were defined to be positive away from the surface. In 2003, a Campbell CR23x data logger was used to log the air temperature, water vapour and 3-axis wind speed fluctuations at 10 Hz. The mean, variance and covariance of these parameters, along with sensible and latent heat flux, were computed using standard equations (Reba *et al.*, 2009), with data stored as 30 min averages. Data filtering was applied to remove spurious data. Reba *et al.* (2009) noted that for snow-covered surfaces, corrections for air density, sensor heating and axis rotation are typically small, and this was confirmed for the present data set by Endrizzi and Marsh (2010).

During the 2003 study period, incoming and outgoing shortwave radiation was measured at each study location using recently calibrated radiometers from various manufacturers (Table I). Although TTS and TUP had similar instruments, a comparison demonstrated unexpected differences. Incoming solar radiation as measured by an Epply B&W pyranometer (model 8–48) at TUP was typically similar in magnitude to that measured by a Kip and Zonen model CNR1 (near the surface) at TTS prior to shrubs partially obstructing the sky view. However, incoming solar radiation measured above the shrub canopy at TTS by a REBS PDS7·1 was consistently lower than either of these, by up to 150 W m^{-2} at higher radiation values. These recently calibrated radiometers were also tested at a control site with similar results, confirming that the differences were not due to alignment issues. The factors controlling these differences are not well understood. In order to ensure a consistent comparison of radiation at each site in 2003, we will use the following combination of radiometers (Table I):

1. The TUP Epply B&W pyranometer was used to represent incoming solar radiation at both TTS and TUP. The similarity in incoming solar radiation at both sites was confirmed using a Kipp and Zonen CNR1 at both sites from 2005 to 2007, when there was a linear relationship between the data with an R^2 of 0·95 and a slope of 0·98 (regression forced through the origin) for the grouped data, and with similar slopes and values of R^2 for each year individually.
2. Outgoing shortwave radiation was estimated from incoming solar radiation multiplied by the albedo, with albedo estimated from the Epply B&W pyranometer for the TUP site, and from REBS PDS7·1 pyranometer for the TTS site. In subsequent years (2005–2007), Kipp and Zonen CNR1 radiometers were used at all sites in order to ensure a consistent data set.
3. Incoming longwave radiation was assumed to be the same at both TTS and TUP (Table I). This was confirmed for the period 2005–2007 using a Kipp and Zonen CNR1 at both sites, when there was a linear relationship between incoming longwave radiation at TUP and TTS with an R^2 of 0·92 and a slope of 1·01 (regression forced through the origin), for grouped data, and similar slopes and values of R^2 found for each year individually.
4. Net radiation was estimated for both TTS and TUP from REBS radiometers, and also calculated from each individual radiation component.

Prior to the start of snowmelt, snow surveys based on extensive land cover were carried out throughout the TVC basin in all study years (2003–2007) following the methods and terrain types of Marsh and Pomeroy (1996), who classified TVC as: 70% tundra, 21% shrub, 8% drifts and 1% forest. Snow surveys were continued at both TTS and TUP throughout the snowmelt period in 2003.

In 2007, a time lapse camera was installed on the TTS tower to provide photographic evidence of changes in snow and shrub characteristics during the melt period. This camera was located at a height of 7·5 m, was angled at approximately 15° below horizontal and was facing north.

To supplement the Marsh and Pomeroy (1996) vegetation classification of TVC, LiDAR (Hopkinson *et al.*, 2008) estimates of vegetation heights were obtained on 19 July 2004. These measurements were acquired with an Optech ALTM 2050 LiDAR system using a Twin Engine Piper Navajo (C-FZHG) aircraft operated by LaserMap Image Plus for Airborne Imaging Inc. Depending on weather conditions, flying height ranged from 1900 to 1200 m above ground, with a pulse rate of 50 000 s^{-1}, a scan rate of between 29 and 32 scans per second, a field of view between +1 and 15–20° and an average spatial sampling of 1·5 m. Global positioning system (GPS) ground control stations were established at the Inuvik

Table I. Instrumentation for the three main study sites (TVC main meteorological—TMM, TVC upper plateau—TUP, and TVC tall shrub—TTS), where z is the height above the surface in m, for 2003–2007

	Instruments	TMM		TUP		TTS	
		Instrument	z (m)	Instrument	z (m)	Instrument	z (m)
	2003 and 2004						
Above canopy	Wind speed/direction	RM Young	10·0	NRG40/—	1·21	2 levels NRG40/NRG200P	9·5, 4·25
	Net radiation	REBS Q7·1	2·62	REBS THRDS7·1 in/out	2·82	REBS THRDS7·1 in/out	5·97
	Incoming shortwave	REBS PDS7·1	2·59	Epply B&W	1·32	REBS PDS 7·1 Used Epply B&W from TUP	5·97
	Outgoing shortwave	REBS PDS7·1	2·59	Epply B&W *Used incoming shortwave × albedo*	1·32	REBS PDS 7·1 *Used TUP incoming shortwave × albedo*	5·97
	Incoming longwave	—	—	*Estimated from incoming longwave from TTS* —	—	Epply PIR	5·85
	Outgoing longwave	—	—	Epply PIR	2·54	*CNR1 ('below' canopy)*—	—
	Albedo			*Estimated from Epply incoming and outgoing shortwave*		*Estimated from REBS incoming and outgoing shortwave*	
	Sensible heat flux	—	—	CSAT3 sonic anemometer	3·20	CSAT3 sonic anemometer	6·48
	Latent heat flux	—	—	KH20 Krypton Hygrometer	3·20	KH20 Krypton Hydrometer	6·48
Near surface	Air temperature/RH	HMP35CF	1·50	HMP35CF	1·29	HMP35CF	1·45
	Barometric pressure	Setra	1·40	—	—	—	—
	Wind speed	—	—	—	—	2 levels NRG40	See above
	Rainfall	Tipping bucket	1·17	Yes	1·10	—	—
	Precipitation	Fischer Porter with nipher shield	2·50	—	—	—	—
	Precipitation	Nipher snow gauge	1·60	—	—	—	—
	Net radiation	—	—	NA	—	Kipp and Zonnen CNR1	1·08
	Incoming shortwave	—	—	NA	—	CNR1	1·08
	Outgoing shortwave	—	—	NA	—	CNR1	1·08
	Incoming longwave	—	—	NA	—	CNR1	1·08
	Outgoing longwave	—	—	NA	—	CNR1	1·08
	2005–2007						
	All instrumentation as in 2003 and 2004, except the following:						
	Incoming/outgoing short and longwave	CNR1	2·39	CNR1	2·82	CNR1	5·56

Note that in italics there is a description of how radiation was estimated when there were problems with the main instrumentation as noted in the text. Lines (—) indict no instrumentation at that location, and NA is not applicable.

airport (45 km to the south) for the southern portion of TVC, and at Swimming Point (50 km to the northwest) for the northern portion of TVC. Real-time kinematic (RTK) GPS surveys from the respective base stations were completed along the runway centre line and profiles perpendicular to the runway in order to identify any roll, pitch and heading misalignment between the IMU (inertial measurement unit) and the sensor. Terrascan analysis software was used to classify terrain types, similar to that of Marsh and Pomeroy (1996), based on vegetation heights, as follows: tundra was defined as areas where the vegetation was less than 0·50 m in height; low shrub tundra where vegetation was greater than 0·50 m and less than 1·25 m; tall shrubs where vegetation was greater than 1·25 m and less than 3·00 m and forests where vegetation height was greater than 3·00 m. Using these height-based classifications, vegetation was mapped at 2·0 m grids over the entire TVC domain (Figure 1).

In the summer of 2005, plant community composition and green alder patch characteristics were surveyed along two transects in an area mapped as tall shrub and two transects located in an area mapped as low shrub. At each transect the percent cover of all vascular plants was estimated using 5 m^2 quadrats ($n = 10$/transect) for tall shrubs, and 0·5 m^2 quadrats for dwarf shrubs and herbs. Nomenclature for vascular plants follows Porsild and Cody (1980) and Catling *et al.* (2005). Green alder stem characteristics were measured in quadrats, located by randomly selecting shrub quadrats (5 m^2) where alder cover was >0 (up to 4/transect). In these quadrats, the height of all individual shrubs, the basal diameter of all alder stems and the basal area occupied by those stems ($cm^2 m^{-2}$) were measured.

The CLASS

The Canadian Landsurface Scheme (CLASS) (Verseghy, 1991; Verseghy *et al.*, 1993) was developed at Environment Canada and is employed in both the Canadian GCM (Flato *et al.*, 2000) and regional climate model (Caya and Laprise 1999; MacKay *et al.*, 2003). The version used in this study (CLASS 3·3) employs a 'big-leaf' canopy representation over three soil layers, with an optional mosaic formulation to represent different surface types in separate patches. Within each patch, the surface is divided into four surface types (bare soil, snow, canopy over bare soil and canopy over snow), which are treated separately. Above a vegetation canopy or in the absence of a canopy, turbulent fluxes of sensible and latent heat are calculated using flux gradient relationships and Monin–Obukhov similarity theory. Under-canopy fluxes are calculated based on free convection (Deardorff, 1972). The snowpack is modelled as an explicit single layer of variable depth and extent. Snow cover is considered complete when the average depth (z_{snow}) exceeds 0·1 m, and at shallower depths the fractional snow-covered area (SCA) is modelled as SCA = z_{snow}/0·1 m. Most of the physical processes related to snow for this model are described in Bartlett *et al.* (2006), and those relevant to this study are briefly outlined below.

Canopy transmissivity (τ_c) is modelled for full-spectrum shortwave radiation and for the visible portion of the spectrum with the near-infrared transmissivity found as a residual (Verseghy *et al.*, 1993). Beer's law relationship is employed, with

$$\tau_c = \exp(-\kappa L) \quad (1)$$

where L is projected leaf area index (LAI) and κ is an extinction coefficient. CLASS models L based on assigned minimum (L_{min}) and maximum (L_{max}) values; $L_{min} > 0$ maintains an effective stem area index in winter (e.g. for trees). A temperature-based algorithm is used to initiate leaf fall (broadleaf) or dormancy (needle leaf) in the autumn and to initiate leaf-out in spring. For clear skies over the full shortwave spectrum, $\kappa_o = 0{\cdot}4$ for fully leaved broadleaf trees, $\kappa_o = 0{\cdot}8/\cos Z$ for leafless broadleaf trees and $\kappa_o = 0{\cdot}4/\cos Z$ for crops and grass, where Z is the solar zenith angle. For the visible range, $\kappa_{o,\ VIS} = 0{\cdot}7$ for fully leaved broadleaf trees, $\kappa_{o,\ VIS} = 0{\cdot}8/\cos Z$ for leafless broadleaf trees and $\kappa_{o,\ VIS} = 0{\cdot}5/\cos Z$ for crops and grass. For cloudy skies, canopy transmissivity is calculated using a weighted average of clear sky values from various zenith angles following Goudriaan (1988), which approximates the effect of the standard overcast distribution of diffuse shortwave radiation of Steven and Unsworth (1980).

The total albedo for a canopy over snow is found as

$$\alpha = \alpha_c(1 - \chi) + \alpha_s(\chi)\tau_c \quad (2)$$

for both the visible and near-infrared bands, where χ is the gap fraction or sky view factor (the fraction of sky visible from below the canopy), α_s is the modelled snowpack albedo, α_c is the canopy albedo found as the weighted average of the snow-covered and snow-free values and τ_c is the canopy transmissivity. CLASS calculates χ using an equation analogous to (1) with an extinction coefficient that varies with vegetation type.

Over time, snowpack metamorphism and melt cause its albedo to decrease. CLASS assumes a fresh snowpack albedo (α_s) of 0·84, which decreases over time as

$$\hat{\alpha}_s(t) = \hat{\alpha}_s(t-1)\exp(-B\Delta t) \quad (3)$$

where $\hat{\alpha}_s = \alpha_s - \alpha_{s,min}$, Δt is the time step and $B = 0{\cdot}01/3600$ is a constant. If no melting occurs during a time step, the minimum snowpack albedo ($\alpha_{s,min}$) is set to 0·7, but if melting occurs it is set to 0·5. New snow refreshes the snowpack albedo back to 0·84. For this study, based on observations at the TVC sites, we changed the model so that fresh snow has an albedo of 0·9 rather than 0·84.

The density of fresh snow ($\rho_{s,f}$) is modelled based on air temperature using a relationship developed by Hedstrom and Pomeroy (1998) from the data of Schmidt and Gluns (1991) and the US Army Corps of Engineers (1956), as $\rho_{s,\ f} = 67{\cdot}92 + 51{\cdot}25e^{T_a/2{\cdot}59}$. For air temperatures ($T_a$) greater than 0 °C, $\rho_{s,\ f} = \min(200,\ 119{\cdot}2 +$

$20T_a$). Snowpack densification is modelled using an empirical relationship with time (Verseghy, 1991), as

$$\widehat{\rho}_s(t) = \widehat{\rho}_s(t-1)\exp(-B\Delta t) \quad (4)$$

where $\widehat{\rho}_s = \rho_s - \rho_{s,\ max}$. In the absence of melting, the following exponential relationship with depth is used (Tabler *et al.*, 1990; Pomeroy *et al.*, 1998):

$$\rho_{s,\ max} = 450 - \frac{204{\cdot}7}{z_{snow}}\left[1 - e^{-z_{snow}/0{\cdot}673}\right],\ T_s < 0\,^{\circ}\mathrm{C} \quad (5)$$

For an isothermal snowpack at 0 °C, the constant 450 kg m^{-3} is replaced by 700 kg m^{-3}. Melt water or rain that freezes in the snowpack has the density of ice and can increase snowpack density (ρ_s) above that of Equations (4) and (5). The snowpack can hold liquid water up to a maximum of 4% of the modelled SWE.

RESULTS

Shrub characteristics and end of winter snow accumulation

The TTS shrub patch, the only large, continuous area of tall shrubs in the TVC area, likely occurs due to a previous tundra fire, as indicated by burned wood located in the upper sections of the soil. Previous studies (Lantz *et al.*, 2010a,b) have shown that tundra fires facilitate the development of dense stands of tall shrub. Field observations show that the TTS site is characterized by an abundance of green alder (*Alnus viridis* ssp. *fruticosa* (Ruprect) Nyman) and diamondleaf willow (*Salix pulchra* Cham.), with the alder shrubs averaging 167 cm in height and a standard deviation of 89 cm, and with a mean basal stem thickness of 2·5 cm and standard deviation of 1·4 cm (Table II). A LiDAR estimate of vegetation height is similar to that given above, with vegetation within 300 m of the TTS tower comprised of a mixture of tundra, low shrubs and tall shrubs. Tall shrubs covered approximately 75% of the area within 300 m of the TTS tower (Figures 3 and 4, and Table II). Tall shrubs had a maximum height of 353 cm (Figure 4), a mean of 153 cm and a standard deviation of 32 cm. The similarity in the estimate of mean vegetation height from field observations (167 cm) and from LiDAR (153 cm) supports the mapping of vegetation heights using LiDAR across the TVC basin as shown in Figure 1.

The vegetation at the TUP tundra site 2·6 km to the north of TTS (Figure 1), and at a similar elevation, was dominated by dwarf birch (*Betula glandulosa* Michx.), fruticose lichens, northern Labrador tea (*Ledum decumbens* (Ait.) Lodd) and cottongrass (*Eriophorum vaginatum* L.) The LiDAR data show that vegetation heights in the vicinity of TUP averaged 9 cm, with a maximum of 53 cm, and a standard deviation of 6 cm (Figure 4).

The large alder shrubs at TTS were not standing upright at the end of winter 2003, but instead were bent over and mostly covered with snow (Figure 2a). The exact cause of this is unknown, but is likely due to a combination of accumulation of snow or hoar frost on the shrub branches, possibly in combination with high winds during the early portions of the winter. The bending of tall shrubs has also been described by Marsh *et al.* (2003) for this site, Sturm *et al.* (2005) in northern Alaska and Pomeroy *et al.* (2006) for an alpine site in the southern Yukon. As the shrubs became bent over at some time

Table II. Shrub characteristics in the vicinity of the TVC tall shrub (TTS) study site

	From field observations	From LiDAR for the 300 m area around TTS tower
Alder shrub height		
Mean (cm)	167	153
Standard deviation (cm)	89	32
Sample size	39	70 477
Tall shrub ground cover		
% of area	70	75
Shrub stem diameter		—
Mean (cm)	2·5	—
Standard deviation (cm)	1·4	—
Sample size	45	—

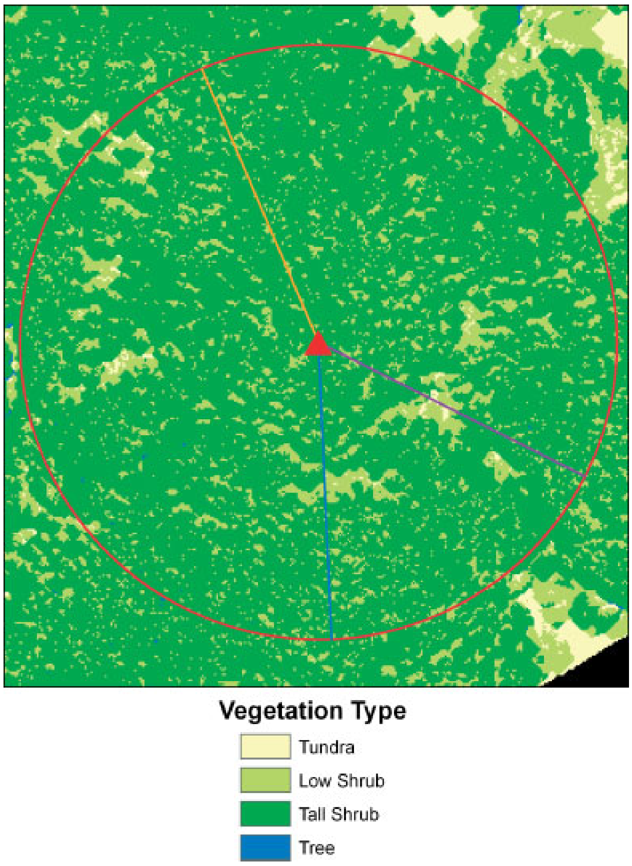

Figure 3. Vegetation classes for 2 m grids surrounding the TTS meteorological tower from LiDAR. Vegetation classes are as defined in Figure 1. The red triangle marks the location of the TTS tower, and the red circle is 300 m in radius centred on the tower. Vegetation height along the three transects are shown in Figure 4. A similar plot for TUP would show the entire area as tundra

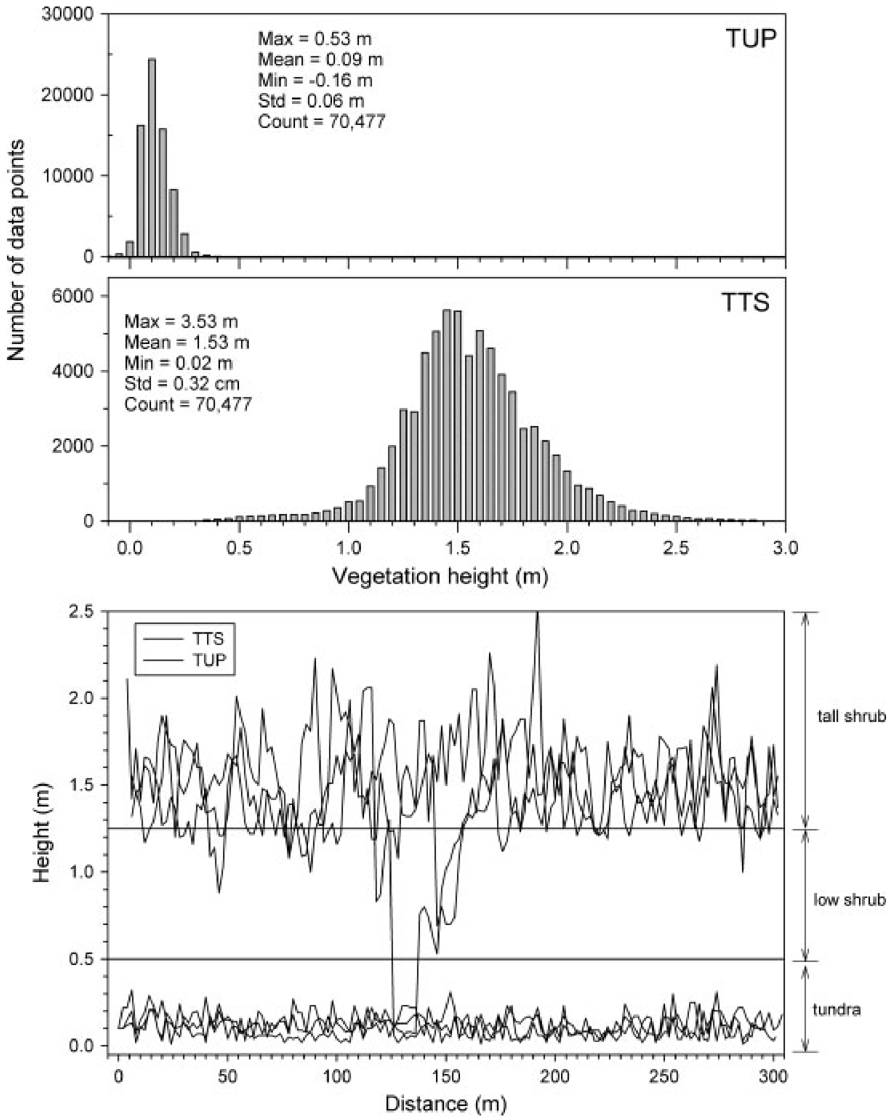

Figure 4. Vegetation heights from LiDAR for (top) entire 300 m zone surrounding the TUP and TTS towers, and (bottom) along three transects for both TTS and TUP

Table III. End of winter snow water equivalent for main terrain types and the weighted mean for each terrain type within TVC

Landcover	% of TVC Area	2003 (mm)	2004 (mm)	2005 (mm)	2006 (mm)	Mean
Tundra	70	99	102	84	204	122
Shrub tundra	21	141	185	133	191	163
Drift	8	499	718	389	696	576
Forest	1.0	155	238	133	192	180
TVC basin mean		141	171	120	242	159

during the winter, and the inter-shrub areas filled with snow, the shrub areas developed properties similar to the tundra site in terms of wind regime, snow accumulation and radiative characteristics. These buried shrubs 'spring-up' over a brief period of time during spring melt, with significant effects on radiation and therefore melt. This process will be described later in more detail.

During the April and 16 April 2003 period when the snow surveys were conducted, less than 2 mm SWE fell as snow. As shown in Table III, tundra had the lowest mean SWE (99 mm), while drift sites had the highest mean SWE with a value of 499 mm. Between these extremes are the shrub tundra with a mean SWE of 141 mm, and forest with a mean SWE of 155 mm. Weighting these values by area, gives a basin mean SWE of 141 mm. Based on Pomeroy *et al*. (1997), who suggested that a TVC open forest site has minimal blowing snow and sublimation, the forest site snow cover should be similar to winter snowfall. This suggests that average basin sublimation for the winter of 2002–2003 was approximately 9% of the winter snowfall. After the basin wide snow surveys were completed on 16 April 2003, when the SWE at TTS and TUP were 115 and 98 mm, respectively, the Fischer–Porter precipitation gauge measured 16 mm of precipitation between 17 April and 19 May, with an additional 2 mm from 19 May to 24 May. The effect of this snowfall, minus any sublimation, on snow accumulation at the study sites was determined by carrying out snow surveys at TTS and TUP during the period leading up to, and throughout the melt period. These snow surveys showed that maximum SWE was 120 mm at TUP on 18 May 2003 and 144 mm at TTS on 19 May 2003. The April snow surveys plus precipitation (114 and 131 mm), is lower than measured snow on the ground on 18 May and 19 May at TUP and TTS by 6 and 13 mm, respectively, suggesting that the Fischer–Porter precipitation gauge underestimated snow fall, as would be expected in a wind blown environment (Goodison *et al.*, 1998).

The average end of winter SWE over the 2003–2006 period, was 159 mm, with values of 122, 163, 576 and 180 mm for the tundra, shrub tundra, drift and forest sites, respectively (Table III). Assuming that the forest, with a mean SWE of 180 mm, was representative of winter snowfall, as suggested by Marsh and Pomeroy (1996), then an average of 12% of the winter snowfall sublimated. The shrub tundra SWE was consistently higher than the tundra but lower than the forest SWE, suggesting that 17 mm of snow is removed from the shrub areas by a combination of blowing snow transport out of the shrubs and/or sublimation during blowing snow. This value is larger than may be expected from a shrub site, and is likely due to the bending over of the shrubs.

CLASS initialization

The CLASS 3·3 simulations were initialized on 12 April 2003, with site properties and model parameters of interest as shown in Table IV. The SWE and snowpack density and albedo were initialized based on snow surveys conducted at each site. Additional snow surveys conducted close to the respective instrument towers on 20 May showed that accumulated SWE was slightly larger around the instrument towers (where radiation and flux measurements were made) than in the surrounding area. This was accounted for by adding 10 and 24 mm to the initial SWE values from the larger snow surveys at TUP and TTS, respectively.

In CLASS the largely non-woody vegetation at TUP was represented as grass, with a minimum LAI (Table IV) set to 1·5 following Verseghy *et al.* (1993), and a maximum LAI of 1·65 determined from model calibration following Kouwen *et al.* (1993) which is similar to values found in the literature for tundra vegetation. The alder and willow shrubs at TTS were each represented as broadleaf trees, but CLASS was modified so that the taller alder shrubs were buried by snow until a prescribed spring-up period (18–26 May), when the height was gradually increased from 0·1 to 2 m. The minimum LAI was 0·9 for alder and 0·6 for willow, and the maximum was 3·2 for alder and 2·0 for willow. The fractional coverage of alder was set to 0·5 and 0·4 for willow. These values were determined from measurements at the site using a LI-COR model LAI-2000 plant canopy analyzer.

Radiation

Shortwave radiation: Early in the 2003 study period, the albedo was very similar at each site (Figure 5), due to the fact that, as described in Section *Shrub Characteristics and End of Winter Snow Accumulation*, the shrubs at TTS were not standing upright at the end of winter, but instead were bent over and mostly covered with snow. Starting on 19 May, the albedo at TTS began to decline (Figure 5) as air temperature rose above 0 °C (Figure 6a), while at TUP the albedo remained nearly constant, or even increased slightly (Figure 5). There was a brief increase in albedo at TTS during a cold period between 25 May and 26 May, after which albedo continued to decline as shrubs were exposed and snow-free areas developed (Figure 5). Albedo at TUP did not begin to decline until

Table IV. Site properties specified for simulations using CLASS 3·3

Parameter	TUP	TTS
Canopy height (m)	0·08	2·0 (alder), 0·6 (willow)
Fractional coverage	1·0	0·5 (alder), 0·4 (willow)
Maximum leaf area index	1·65	3·2 (alder), 2·0 (willow)
Minimum leaf area index	1·5	0·9 (alder), 0·6 (willow)
Visible canopy albedo	0·07	0·04 (alder), 0·05 (willow)
Near infrared canopy albedo	0·35	0·15 (alder and willow)
Longwave emissivity (snow, soil, vegetation)	1·0	1·0
Biomass density (kg m^{-2})	0·2	5·8 (alder), 2·0 (willow)
Soil texture layer 1	Fibric peat	Fibric peat
Soil texture layer 2	Hemic peat	Hemic peat
Soil texture layer 3	35% sand, 40% clay	35% sand, 40% clay
Initial SWE (mm)	108	127
Initial ρ_{snow} (kg m^{-3})	230	190
Initial snowpack albedo	0·90	0·90

Note that minimum leaf area index is used to represent the plant area index outside of the growing season.

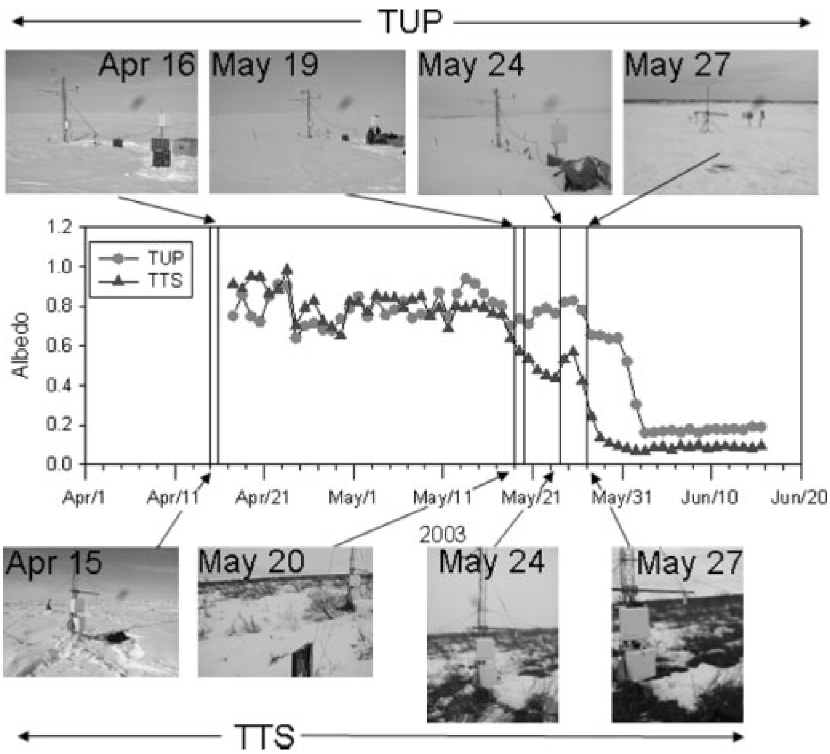

Figure 5. Change in albedo over the snowmelt period at both TUP and TTS. Also shown are photos of each site during the melt period showing the shrubs at TTS emerging from the snow cover

the start of the main melt period after 26 May when air temperature again rose above 0 °C. This earlier decline in albedo at TTS resulted in lower reflected shortwave radiation and therefore higher net shortwave radiation at TTS compared to TUP throughout the melt period (Figure 6d). By the end of melt, the albedo was very similar at both sites (Figures 5 and 6b), with TUP having slightly higher albedo, and therefore very similar but slightly lower net shortwave radiation as well.

This same pattern in albedo (Figure 7) and net shortwave radiation was observed in 2005–2007. In all years, the albedo at TTS began to decrease first, with the albedo continuously higher at TUP during the melt period. As in 2003, the pre-melt albedos at TUP and TTS were similar in 2006. However, for much of the pre-melt period in 2005 and 2007, the albedo was lower at TTS than at TUP. This was due to the fact that in 2005 and 2007 the shrubs were more erect, with more shrubs extending above the snow surface than in 2003 and 2006 (Figure 7).

Although the slow emergence of the shrubs from the snow over a period of many days at TTS was not documented in detail during 2003, a series of time lapse photographs in 2007 clearly show this process (Figure 8). Between 18 May and 22 May 2007, the shrubs within the photographic scene were bent over and mostly snow covered, with only small portions of the shrubs extending above the snow. After 23 May, the shrubs were gradually released from the snow and became more erect, nearly reaching their final form by approximately 30 May. This emergence of the shrubs from the snowpack is likely related to a decrease of snow depth and strength over the melt period, in combination with an increase in the elasticity of the shrub stems as they warm (Sturm *et al.*, 2005; Pomeroy *et al.*, 2006). When fully emerged, these alder shrubs originate from a small centre point and angle outwards, with the first areas of snow-free ground appearing on 28 May as patches near the base of the shrubs. These snow-free patches then expand in area.

Longwave radiation: Outgoing longwave radiation at TUP and TTS (below canopy) were similar at both sites in 2003 (Figure 9b). As there was no downward-facing pyrgeometer above the shrub canopy in 2003, the above canopy radiation regime is unknown for 2003. However, data for 2005–2007 shows that the outgoing longwave was similar at both sites for much of the observation period, but during the melt periods outgoing longwave at TTS was typically higher than at TUP (Figure 10). These data are consistent with field observations which showed that the shrubs were released from the snow during this period and that shrub stems had temperatures much higher than the air temperature or the snow surface.

CLASS simulation: The results of the CLASS simulation show reasonable agreement with the observed albedo before and after the melt at both of the sites (Figure 6b). The albedo decreased rapidly at TUP as the snow-free area increased and this is captured reasonably well by the model. At TTS, the decrease in albedo caused by the shrubs springing up is captured, but the model lags the observations in the latter part of the melt period (26 May to 2 June) because, as will be shown, the SCA decreases more slowly in the model than in observations.

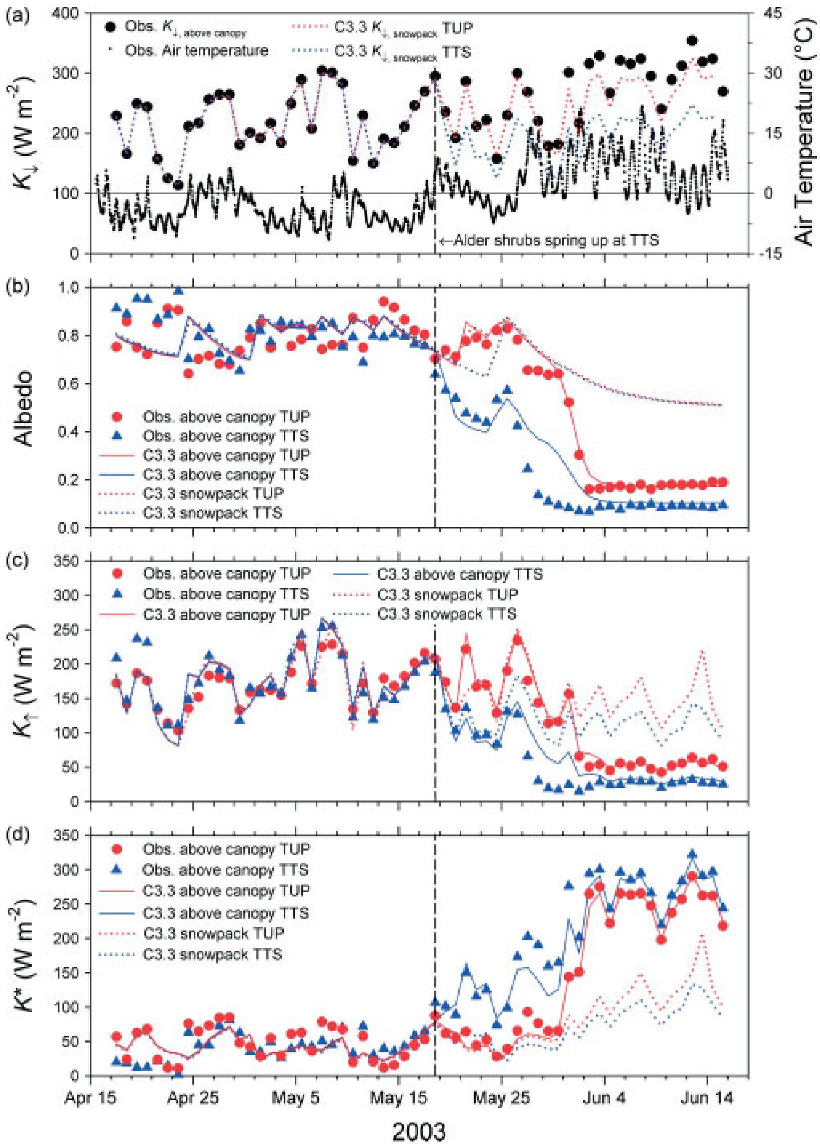

Figure 6. Observed and simulated incoming, outgoing and net solar radiation, and albedo at TUP and TTS. Also shown is observed air temperature at TTS

The effects of the changed albedo are manifest in the reflected shortwave radiation as well as net shortwave radiation K^*. Patterns of observed and modelled K^* were similar at both sites before the uncovering of the shrubs at TTS (Figure 6d), after which they were always larger at TTS. Differences between the sites were largest during the melt period before the shorter vegetation at TUP was uncovered. During the main melt period (20 May to 2 June) observed differences in K^* averaged 79 W m^{-2} or 6·8 MJ m^{-2} day^{-1}, and approached 100 W m^{-2} or 8·6 MJ m^{-2} day^{-1} on sunny days while modelled differences averaged 73 W m^{-2} or 6·3 MJ m^{-2} day^{-1}. Modelled outgoing longwave radiation also follows the pattern of observed values at TUP quite well (Figure 9b). At TTS, modelled values are similar to those at TUP prior to the uncovering of the shrubs, and are always larger afterwards. The largest differences occurred during the primary melt period because the tall shrubs are warmer than the snowpack that they partially obscure. Modelled differences averaged 15 W m^{-2} or 1·3 MJ m^{-2} day^{-1} from 20 May to 2 June. The combined effect of increased shortwave absorption and increased longwave emission at TTS can be examined through their effect on net radiation. Figure 9d shows that during the peak melt period (20 May to 2 June) the modelled net radiation was larger at TTS by an average of 58 W m^{-2} or 5 MJ m^{-2} day^{-1}, showing a significant net radiative gain during the melt period at TTS relative to TUP.

Prior to the shrubs springing up, the observed net solar radiation was similar at TUP and TTS (Figure 6d), after which the Kipp and Zonen CNR1 sensor at TTS was within the canopy. As far as snow melt is concerned, an important factor controlling melt is the reduction in shortwave radiation incident on the snowpack caused by shading by the shrub canopy at TTS versus the additional contribution to the downward flux of longwave radiation caused by emission from the canopy. The Kipp and Zonen CNR1 was mounted at 1·08 m, and as a result was not able to provide a representative measurement of under canopy radiation because a significant part of the

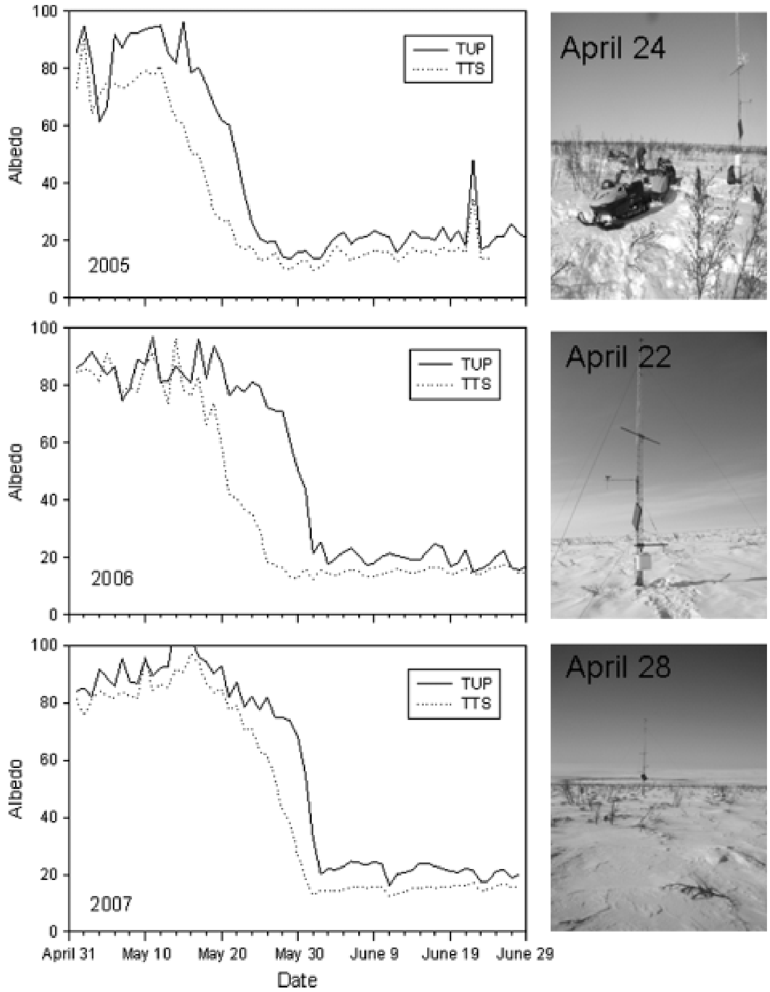

Figure 7. Albedo at TUP and TTS, above 'canopy' during the 2005, 2006 and 2007 melt periods. Photos show snow and shrub conditions in late April of each year

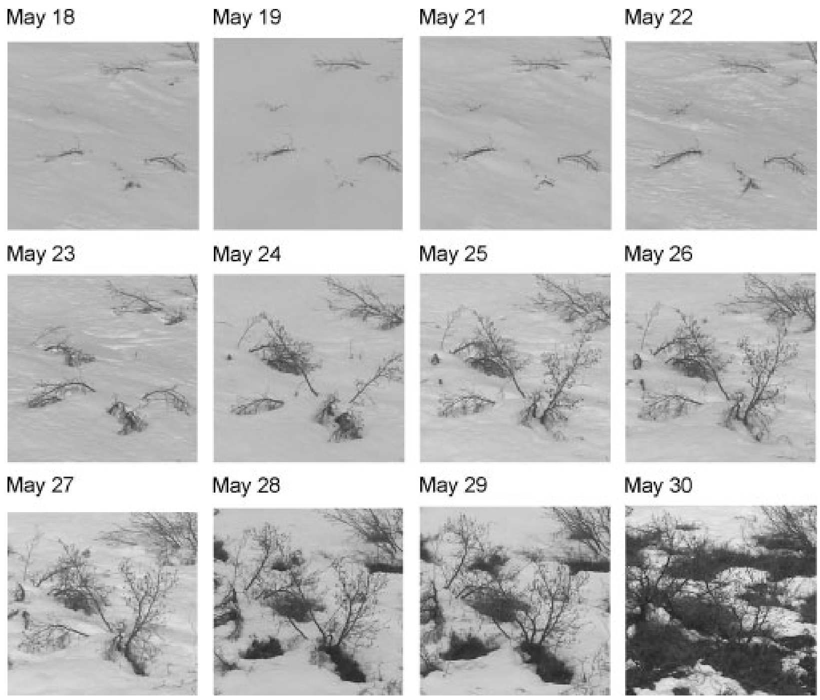

Figure 8. Time lapse photographs of shrubs at TTS in May 2007 showing the gradual emergence of the shrubs from the snow cover, and that the first areas of snow-free ground appear as patches near the base of the shrubs. These snow-free patches then expand in area

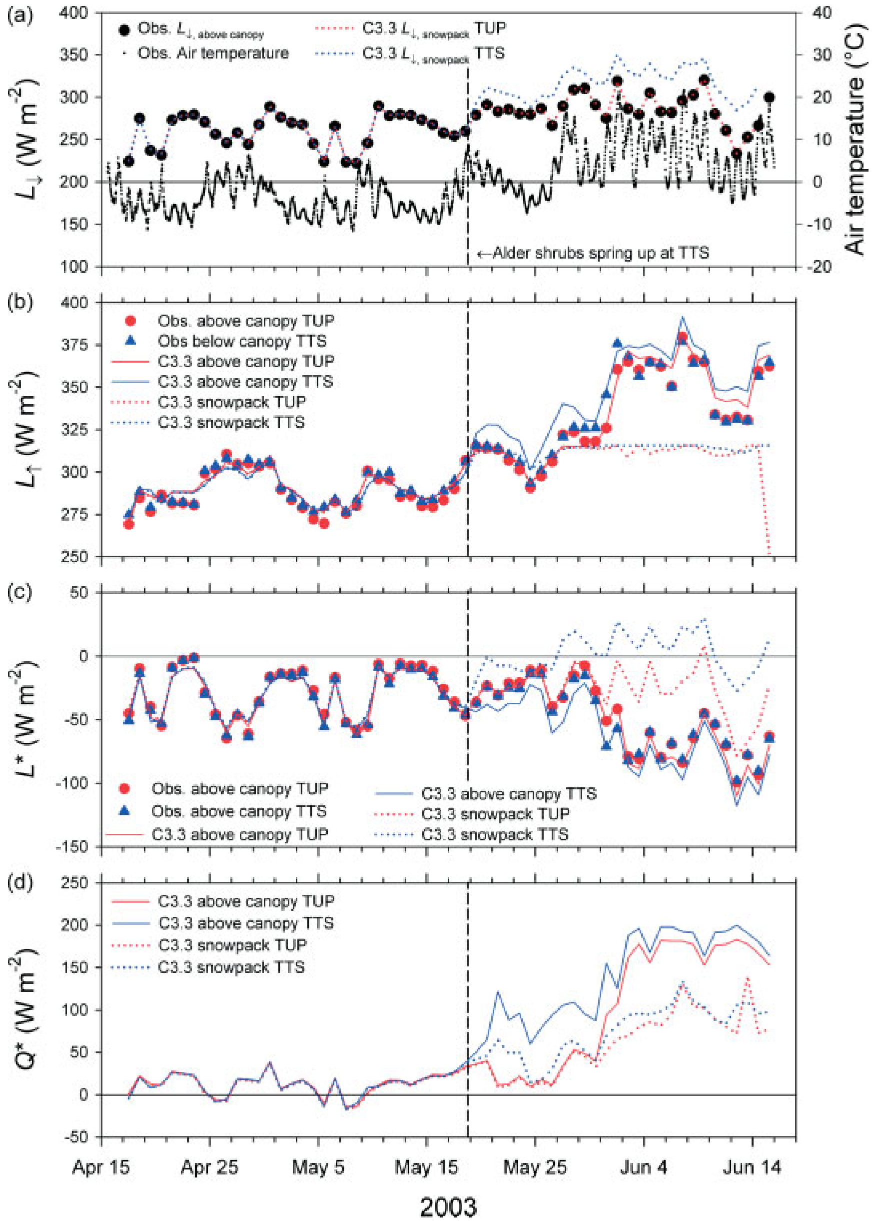

Figure 9. Observed and simulated incoming, outgoing and net longwave radiation and simulated net radiation at TUP and TTS. Observed incoming longwave radiation from TTS above canopy is used for both sites as no incoming measurement was made at TUP in 2003

lower and upper canopy were in the field of view of the downward- and upward-facing sensors. In addition, due to the heterogeneity of the shrubs, a single point measurement would not be representative of the site. Following the shrubs springing up, values of K^* from the CNR1 are larger than the above-canopy values at TTS until the vegetation at TUP is uncovered, when values become quite similar until after June 19 when we presume an increasing leaf area at TTS begins to increase shading at TTS relative to TUP. Modelled K^* above the snowpack at TTS increases slightly relative to TUP despite the larger LAI at TTS because the modelled snowpack albedo is lower at TTS from 20 May to 25 May. Following this, modelled K^* over the snowpack is smaller at TTS until the snowpack is essentially depleted (Figure 6d). The additional shading at TTS resulted in a smaller modelled daily average value of K^* over the snowpack of 12 W m^{-2} or about 1 MJ m^{-2} day^{-1} relative to TUP. Observed daily average values of net longwave radiation (L^*) at 1·08 m at TTS were 5–20 W m^{-2} smaller than above-canopy values at TUP, and did not show an obvious change following the shrubs springing up; however, this may be a result of changes in both upward and downward longwave radiation at TTS following the shrubs springing up, or of the upward-facing sensor seeing too little of the canopy and the downward-facing sensor seeing too much canopy to provide a reliable assessment. Modelled values show an increase in L^* (Figure 9c) at TTS relative to TUP following the shrubs springing up, with daily average values being 22·6 W m^{-2} or 1·9 MJ m^{-2} day^{-1} larger. If we consider the extra incoming longwave radiation received at the snowpack because of emission from the canopy, model results show a daily average additional contribution from the canopy at TTS during the period of 20 May

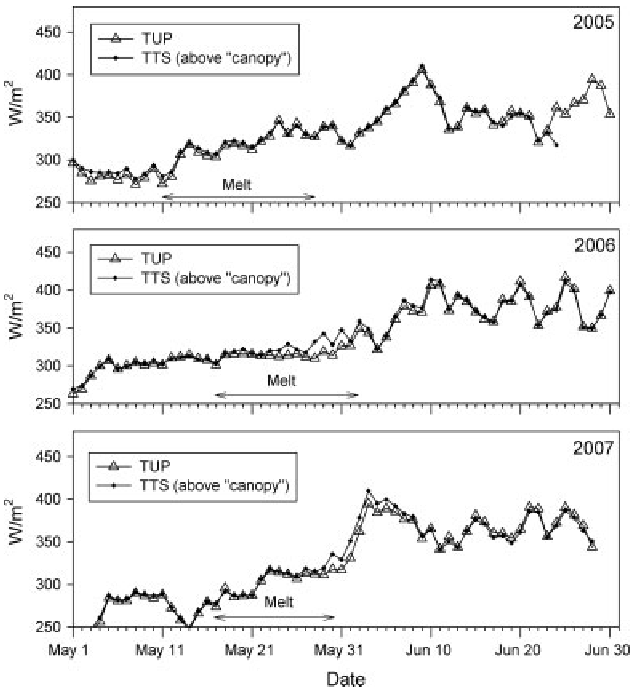

Figure 10. Outgoing longwave radiation at TUP and TTS (above 'canopy') for 2005, 2006 and 2007. Note the increased longwave during the snowmelt period when the shrubs are above the snow, but both sites are still snow covered

to 2 June of 28·7 W m^{-2} or 2·5 MJ m^{-2} day^{-1} versus 0·8 W m^{-2} or 0·07 MJ m^{-2} day^{-1} at TUP. The result is an increase in net radiation over the snowpack at TTS relative to TUP of 10·6 W m^{-2} or 0·9 MJ m^{-2} day^{-1}.

TURBULENT FLUXES OF SENSIBLE AND LATENT HEAT

The sensible heat flux was consistently higher at the shrub site (TTS) than the tundra site (TUP) (Figure 11a), except for a few short periods. Although the latent heat flux (Figure 11b) at TTS was similar to that at TUP during the pre-melt and both melt periods (using air temperature above freezing as a proxy for melt), during the period 22 May to 26 May the latent heat flux was higher at TTS, and then higher at TUP after all of the snow was removed.

During the second melt period between 26 May and 2 June the sensible heat flux increased at both sites, with fluxes at TTS being considerably larger than at TUP. At TTS, the fluxes in this main melt period (Figure 11a and b) were consistently positive, while at TUP they were negative early in the melt period (i.e. towards the snow surface), but became positive by 29 May when SCA at TUP reached approximately 65% (Figure 12a).

The increased sensible heat flux at the shrub site is related to the increased net radiation due to the lower albedo of the shrub/snow surface than that for the tundra snow surface. It must be noted that these turbulent fluxes are those measured above the shrub canopy, not at the snow surface below the shrub canopy. As a result they are not directly related to snowmelt, with the fluxes being used for a combination of warming the shrub trunks/stems and for snowmelt. This increase in turbulent fluxes for shrub areas has important implications for both snowmelt hydrology and atmospheric conditions.

Modelled fluxes of sensible and latent heat show a similar pattern of increasing magnitude, partly due to the increasing magnitude of incoming solar and longwave radiation through the spring, and mainly because of the increase in available energy following the removal of the snowpack. Both sensible and latent heat fluxes were small and of similar magnitude at the two sites prior to the melt when the shrubs at TTS were buried. Sensible heat flux increased immediately following the shrubs springing up at TTS, while at TUP (as in the observed fluxes), this flux was often downwards during the primary melt period towards the unobstructed snowpack surface. Following the melt, the modelled sensible heat flux was slightly larger at TUP while the latent heat flux was larger at TTS but the values were in a similar range.

When we examine the modelled fluxes at the snowpack surface (Figure 13), we see that both fluxes are towards the snowpack (i.e. negative) more frequently during the melt at TUP than at TTS. The larger canopy at TTS, which began to be uncovered 13 days earlier than at TUP, sheltered the snowpack from turbulent heat exchange. This reduction is reasonable as the observed wind speed is lower below the shrub canopy (Figure 11d). However, CLASS does not estimate the below canopy wind speed, but instead models Qh and Qe below the canopy were based on free convection. This probably represents flux values as would be observed below a dense canopy, and as a result actual flux values are likely larger than modelled fluxes below the TVC shrub canopy.

Snowmelt

As noted earlier, the shrub site had a higher maximum SWE prior to melt, than did the tundra site. However, the mean SWE at the shrub site decreased faster than at the tundra site (Figure 12a), suggesting a higher melt rate at the shrub site compared to the tundra site. In addition, the SCA decreased faster at the shrub site than for the tundra site (Figures 5 and 12).

In the simulation, the main snowmelt begins at the same time at both sites; however, the melt proceeds more rapidly in the initial period (Figure 12a) following the shrubs springing up at TTS. The presence of the uncovered shrubs allowed the melt to continue more rapidly at TTS during much of the cold period when air temperatures were below freezing, and is when the bulk of the additional melt at TTS occurred. In fact, the modelled SWE (Figure 12a) suggests that the presence of the tall shrubs affected the SWE at TTS with a decrease in SWE to a value similar to TUP, after which melt proceeded at a similar rate at both sites. During melt, the simulations show (Figure 14) that some melt water infiltrates and subsequently refreezes within the soil column. However, following the disappearance of the snowpack, melt within the soil column ramps up to a

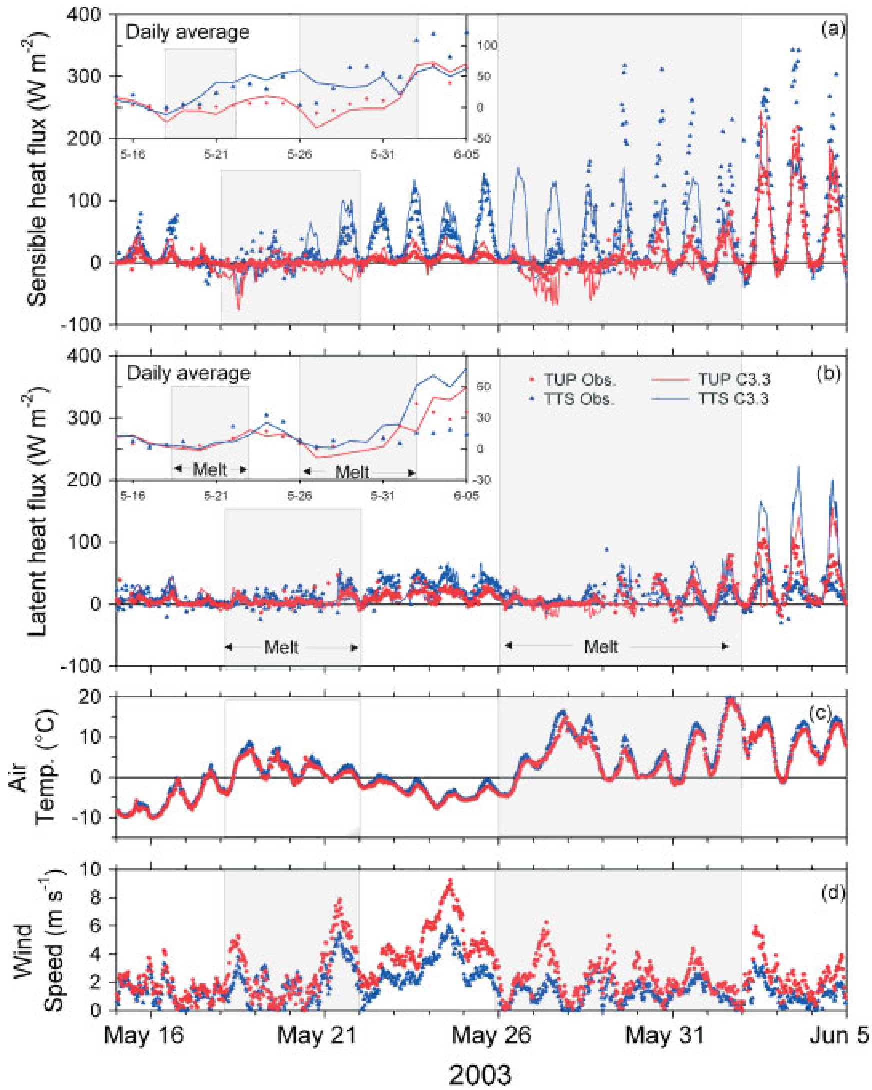

Figure 11. Sensible and latent heat flux for both TUP and TTS. Also shown are the air temperature and wind speed at the study sites. Melt events are defined as those periods with air temperature above 0 °C

magnitude approaching that of the snowpack during the main snowmelt period.

The fractional SCA decreases more quickly with respect to snow depth at TTS, suggesting that patchiness originating around clumps of shrubs and the resulting horizontal advection play a role in the melt. The clumped nature of shrubs and the resulting patchiness in the melt process is not represented in the model, nor is horizontal advection represented. Although some effects of the shrub canopy, such as sheltering from turbulent exchange, increased extinction of shortwave radiation and emission of longwave radiation, are represented, local effects such as the development of melt wells and horizontal patchiness are not represented, and it is likely these effects that are responsible for the more rapid decrease in SCA at TTS.

CONCLUSION

As suggested by Sturm *et al.* (2001a) and Liston *et al.* (2002), the snow accumulation and energy fluxes during melt, were significantly different at a shrub site compared to a nearby tundra site. SWE at the shrub site was approximately 40% higher than at the tundra site, and was only 9% lower than the estimated winter snowfall. Loss of snow due to both transport from the shrub site to nearby accumulation areas, and due to sublimation, was likely enhanced because the shrubs were bent over and covered by snow at some point during the winter.

Shrub cover impacts the fluxes to the snow surface; hence, melt rates in a number of ways. For example, the snowmelt rate was higher at the shrub site than at the tundra site, which resulted in the snow cover being removed at approximately the same time at both sites. This increased melt rate at the shrub site was due to a number of factors.

First, differences between the two sites were only observed once the shrubs began to emerge above the snow surface, indicating that models used to consider the effects of shrubs require a parameterization for shrub burial and exposure. Once they were above the snow surface, modelled turbulent fluxes at the snow surface

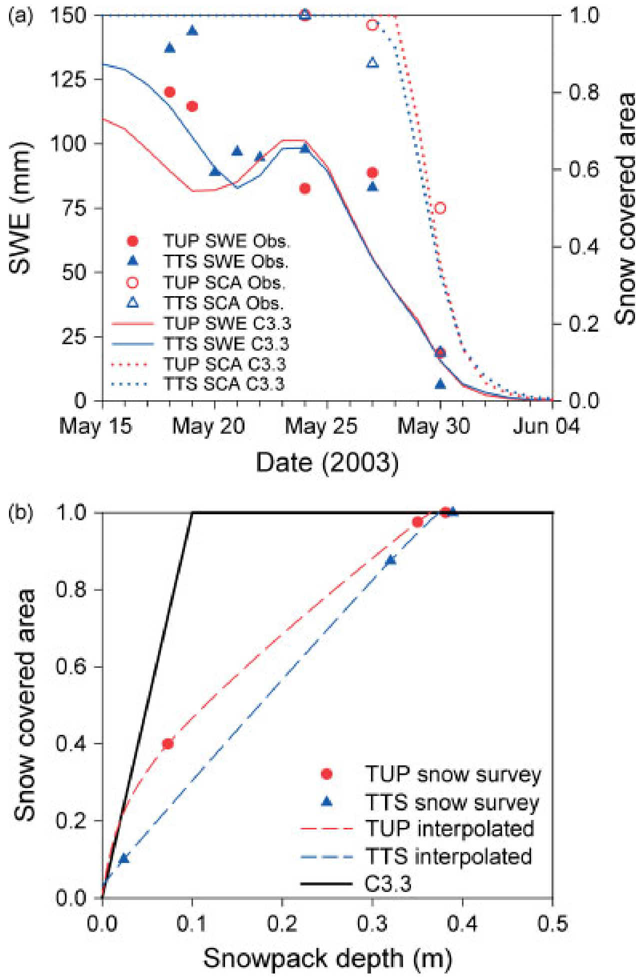

Figure 12. (a) Change in snow water equivalent and snow-covered area during the 2003 melt season for both tundra and alder shrub sites. Melt events are defined as those periods with air temperature above 0 °C. (b) Simulated and observed change in snow-covered area as a function of snow depth

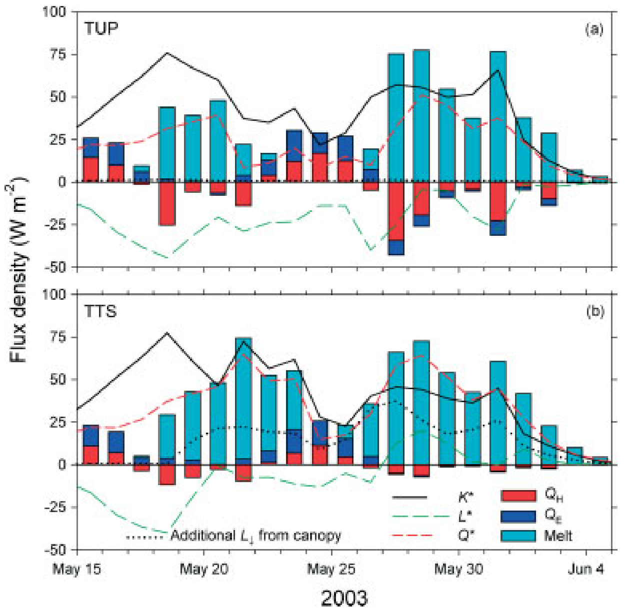

Figure 13. Modelled net shortwave, net longwave and net radiation, sensible and latent heat fluxes, additional longwave radiation received from the vegetation canopy at the snowpack surface and snowmelt, using CLASS 3·3 at TUP and TTS

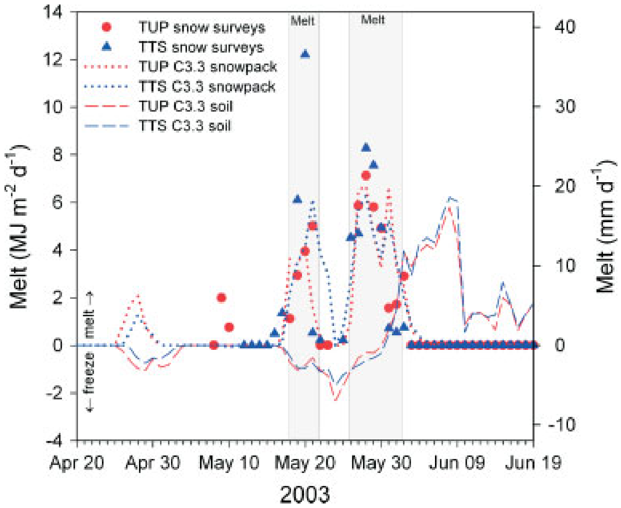

Figure 14. Daily melt rate estimated from snow surveys, and modelled melt/freeze rate in the snowpack and soil using CLASS 3·3. Melt rates estimated from snow surveys were partitioned between surveys using net radiation when the observed air temperature and radiative surface temperature were greater than −1 °C and net radiation was positive

were lower at the shrub site than at the tundra site due to differences in wind speed, with decreased wind below the shrub 'canopy'. In addition, incoming solar radiation was reduced at the snow surface by the shrubs due to shading by the shrub branches. In contrast to this, longwave radiation at the shrub snow surface was higher than that at the tundra site due to emissions from the warm shrub branches. Modelling in conjunction with observations suggests that the increased longwave radiation beneath the shrub 'canopy' is greater than the reduced turbulent fluxes and solar radiation. Ongoing analysis will consider the relative importance of these various factors, and compare to similar observations beneath forest canopies (Sicart *et al*., 2004). These large differences in snow accumulation and melt between shrub and tundra surfaces, demonstrate that additional model experiments are required to consider both the local and regional hydrological effects of future shrub proliferation in existing tundra areas of the Arctic.

In addition to the affects of shrubs on snow processes and hydrology, they also affect the fluxes between the surface and the atmosphere. Outgoing shortwave radiation is reduced, while longwave radiation and sensible heat flux are increased at the shrub site once the shrubs are exposed. Latent heat exchanges during the melt period are similar at the shrub and tundra site. This large difference in energy exchanges demonstrates the need for additional regional climate model studies to consider the effect of future shrub proliferation on regional climate.

ACKNOWLEDGEMENTS

We would like to acknowledge funding from the Climate Change Action Fund, Environment Canada's National

Water Research Institute and the Polar Continental Shelf Project. Essential logistical support has been provided by the Polar Continental Shelf Project and the Aurora Research Institute. Thanks to Cuyler Onclin, Mark Russell, Heather Haywood and Brock McLeod for providing essential field support and data analysis.

REFERENCES

ACIA. 2005. *Arctic Climate Impact Assessment*, Cambridge University Press: Cambridge; 1042.

Bartlett PA, MacKay MD, Verseghy DL. 2006. Modified snow algorithms in the Canadian land surface scheme: model runs and sensitivity analysis at three boreal forest stands. *Atmosphere–Ocean* **44**: 207–222.

Bewley D. 2006. *Shrub-tundra effects on snowmelt energetics and the atmospheric interaction with snow*. Ph.D. Thesis, University of Wales; 196.

Burn CR, Kokelj SV. 2009. The environment and permafrost of the Mackenzie Delta area. *Permafrost and Periglacial Processes* **20**: 83–105.

Catling PM, Cody WJ, Mitrow G. 2005. A compilation of additions to the flora of the continental portions of the Northwest Territories and Nunavut. *Botanical Electronic News* 353.

Caya D, Laprise R. 1999. A semi-implicit, semi-Lagrangian regional climate model: the Canadian RCM. *Monthly Weather Review* **127**: 341–362.

Chapin FS, Shaver GR, Giblin AE, Nadelhoffer KJ, Laundre JA. 1995. Responses of arctic tundra to experimental and observed changes in climate. *Ecology* **76**: 694–711.

Corns IGW. 1974. Arctic plant communities east of Mackenzie-Delta. *Canadian Journal of Botany* **52**: 1731–1745.

Deardorff JW. 1972. Parameterization of the planetary boundary layer for use in general circulation models. *Monthly Weather Review* **100**: 93–106.

Endrizzi S, Marsh P. 2009. Spatial variability of turbulent fluxes and snowmelt energetics due to landscape heterogeneity in an arctic environment. In *17th International Northern Research Basins Symposium and Workshop Iqaluit-Pangnirtung-Kuujjuaq, Canada, August 12 to 18, 2009*; 75–85.

Endrizzi S, Marsh P. 2010. Observations and modelling of turbulent fluxes during melt at the shrub-tundra transition zone 1: point scale variations. *Hydrology Research* in press.

Epstein HE, Beringer J, Gould WA, Lloyd AH, Thompson CD, Chapin FS, Michaelson GJ, Ping CL, Rupp TS, Walker DA. 2004. The nature of spatial transitions in the Arctic. *Journal of Biogeography* **31**: 1917–1933.

Essery R, Pomeroy JW. 2004. Vegetation and topographic control on wind-blown snow distributions in distributed and aggregated simulations for an Arctic tundra basin. *Journal of Hydrometeorology* **5**: 735–744.

Essery R, Li L, Pomeroy JW. 1999. A distributed model of blowing snow over complex terrain. *Hydrological Processes* **13**: 2423–2438.

Flato GM, Boer GJ, Lee WG, McFarlane NA, Ramsden D, Reader MC, Weaver AJ. 2000. The Canadian centre for climate modeling and analysis global coupled model and its climate. *Climate Dynamics* **16**: 451–467.

Goetz SJ, Bunn AG, Fiske GJ, Houghton RA. 2005. Satellite-observed photosynthetic trends across boreal North America associated with climate and fire disturbance. *Proceedings National Academy Sciences* **102**: 13521–13525.

Goodison BE, Louie PYT, Yang D. 1998. *WMO Solid Precipitation Measurement Intercomparison Final Report*. WMO Instruments and Observing Methods Report No. 67, WMO/TD No. 872.

Goudriaan J. 1988. The bare bones of leaf-angle distribution in radiation models for canopy photosynthesis and energy exchange. *Agricultural and Forest Meteorology* **43**: 155–169.

Hedstrom NR, Pomeroy JW. 1998. Measurements and modelling of snow interception in the boreal forest. *Hydrological Processes* **12**: 1611–1625.

Heginbottom JA, Dubreuil MA. 1995. *Canada—Permafrost in National Atlas of Canada*, 5th edn, Plate 2·1 (MCR 4177), scale 1 : 7500,000.

Hopkinson C, Pietroniro A, Pomeroy JW. 2008. Hydroscan: airborne laser mapping of hydrological features and resources. *Environment Canada* 376.

Kouwen N, Soulis ED, Pietroniro A, Donald J, Harrington RA. 1993. Grouped response units for distributed hydrologic modelling. *Journal of Water Resources Planning and Management, ASCE* **119**(3): 289–305.

Lantz TC, Kokelj SV. 2008. Increasing rates of retrogressive thaw slump activity in the Mackenzie Delta region, NWT, Canada. *Geophysical Research Letters* **35**: L06502. DOI: 10.102912007GL032433.

Lantz TC, Kokelj SV, Gergel SE, Henry GHR. 2009. Relative impacts of disturbance and temperature: persistent changes in microenvironment and vegetation in retrogressive thaw slumps. *Global Change Biology* **15**: 1664–1675.

Lantz TC, Gergel SE, Kokelj SV. 2010a. Spatial heterogeneity in the shrub tundra ecotone in the Mackenzie Delta Region, NWT: implications for arctic environmental change. *Ecosystems* **13**: 194–204.

Lantz TC, Gergel SE, Henry GHR. 2010b. Response of green alder (Alnus viridis subsp. fruticosa) and plant community composition to fire and regional climate in Northwestern Canada. *Journal of Biogeography* in press. DOI = 1111/j.1365-2699.2010.02317.x.

Liston GE, McFadden JP, Sturm M, Pielke RA. SR 2002. Modelled changes in arctic tundra snow, energy and moisture fluxes due to increased shrubs. *Global Change Biology* **8**: 17–32.

MacKay JR. 1995. Active layer changes (1968 to 1993) following the forest-tundra fire near Inuvik, NWT, Canada. *Arctic and Alpine Research* **27**: 323–336.

MacKay JR. 1998. Pingo growth and collapse, Tuktoyaktuk Peninsula area, western Arctic coast, Canada: along term field study. *Geographie Physique et Quaternaire* **52**: 271–323.

MacKay JR. 1999. Periglacial features developed on the exposed lake bottoms of seven lakes that drained rapidly after 1950, Tuktoyaktuk Peninsula Area, Western Arctic Coast, Canada. *Permafrost and Periglacial Processes* **10**: 39–63.

MacKay MD, Seglenieks F, Verseghy D, Soulis ED, Snelgrove KR, Walker A, Szeto K. 2003. Modeling Mackenzie Basin surface water balance during CAGES with the Canadian regional climate model. *Journal of Hydrometeorology* **4**: 748–767.

Marsh P, Onclin C, Neumann N. 2002. Water and energy fluxes in the lower Mackenzie Valley, 1994/95. *Atmosphere–Ocean* **4**: 245–256.

Marsh P, Onclin C, Russell M, Pohl S. 2003. Effects of shrubs on snow processes in the vicinity of the Arctic treeline in NW Canada. Northern Research Basins. In *14th International Symposium and Workshop. Kangerlussuaq/Sdr. Strømfjord, Greenland*. August 25–29; 113–118.

Marsh P, Pomeroy JW. 1996. Meltwater fluxes at an arctic forest-tundra site. *Hydrological Processes* **10**: 1383–1400.

Marsh P, Pomeroy J, Pohl S, Quinton W, Onclin C, Russell M, Neumann N, Pietroniro A, Davison B, McCartney S. 2007. Snowmelt processes and runoff at the Arctic treeline: 10 years of MAGS research. In *Cold Region Atmospheric and Hydrologic Studies*, Woo M-K (ed). The Mackenzie GEWEX Experience: Berlin, Heidelberg, New York.

Olthof I, Pouliot D, Latifovic R, Chen WJ. 2008. Recent (1986–2006) vegetation-specific NDVI trends in Northern Canada from satellite data. *Arctic* **61**: 381–394.

Pohl S, Marsh P. 2006. Modelling the spatial–temporal variability of spring snowmelt in an arctic catchment. *Hydrological Processes* **20**: 1773–1792.

Pomeroy JW, Marsh P, Gray DM. 1997. Application of a distributed blowing snow model to the Arctic. *Hydrological Processes* **11**: 1451–1464.

Pomeroy JW, Gray DM, Shook KR, Toth B, Essery RHL, Pietroniro A, Hedstrom N. 1998. An evaluation of snow accumulation and ablation processes for land surface modelling. *Hydrological Processes* **12**: 2339–2367.

Pomeroy JW, Bewley DS, Essery RLH, Hedstrom NR, Link T, Granger RJ, Sicart JE, Ellis CR, Janowicz JR. 2006. Shrub tundra snowmelt. *Hydrological Processes* **20**: 923–941.

Pomeroy JW, Gray DM, Marsh P. 2007. Studies on snow redistribution by wind and forest snow-cover and depletion and frozen soil infiltration in northern and western Canada. *Cold Region Atmospheric and Hydrologic Studies. The Mackenzie GEWEX Experience*, *Hydrologic Processes*, vol. 2. Spring: Berlin; 81–96.

Porsild AE, Cody WJ. 1980. *Vascular Plants of Continental Northwest Territories, Canada, National Museum of Natural Sciences, National Museums of Canada, Ottawa*. 667.

Reba ML, Link TE, Marks D, Pomeroy J. 2009. As assessment of corrections for eddy covariance measured turbulent fluxes over snow in mountain environments. *Water Resources Research* **45**: DOI: 10.1029/2008WR007045.

Schmidt RA, Gluns DR. 1991. Snowfall interception on branches of three conifer species. *Canadian Journal of Forest Research* **21**: 1262–1269.

Sicart JE, Pomeroy JW, Essery RLH, Hardy J, Link T, Marks D. 2004. A sensitivity study of daytime net radiation during snowmelt to forest canopy and atmospheric conditions. *Journal of Hydrometeorology* **5**: 774–784.

Steven MD, Unsworth MH. 1980. The angular distribution and interception of diffuse solar radiation below overcast skies. *Quarterly Journal of the Royal Meteorological Society* **106**: 57–61.

Strack JE, Pielke RA, Sr., Liston GE. 2007. Arctic tundra shrub invasion and soot deposition: consequences for spring snowmelt and near-surface air temperatures. *Journal of Geophysical Research* **112**: DOI: 10.1029/2006JG000297.

Sturm M, McFadden JP, Liston GE, Chapin RS, *III*, Racine CH, Holmgren J. 2001a. Snow-shrub interactions in Arctic Tundra: a hypothesis with climatic implications. *Journal of Climate* **14**: 336–344.

Sturm M, Racine C, Tape K. 2001b. Increasing shrub abundance in the Arctic. *Nature* **411**: 546–547.

Sturm M, Douglas T, Racine C, Liston GE. 2005. Changing snow and shrub conditions affect albedo with global implications. *Journal of Geophysical Research* **110**: DOI: 10.1029/2005JG000013.

Tabler RD, Pomeroy JW, Santana BW. 1990. Drifting Snow. In *Cold Regions Hydrology and Hydraulics*, Ryan WL, Crissman RD (eds). American Society of Civil Engineering: New York; 95–146.

Tape K, Sturm M, Racine C. 2006. The evidence for shrub expansion in Northern Alaska and the Pan-Arctic. *Global Change Biology* **12**: 686–702. DOI: 10.111/j.1365–2486.2006.01128.

US Army Corps of Engineers. 1956. *Snow hydrology: summary report of the snow investigations, North Pacific Division, Portland, Oregon*; 437.

Verseghy DL. 1991. CLASS—a Canadian land surface scheme for GCMs. I: soil model. *International Journal of Climatology* **11**: 111–133.

Verseghy DL, McFarlane NA, Lazare M. 1993. CLASS—a Canadian land surface scheme for GCMs. II: vegetation model and coupled runs. *International Journal of Climatology* **13**: 347–370.

Walker MD, Wahren CH, Hollister RD, Henry GHR, Ahlquist LE, Alatalo JM, Bret-Harte MS, Calef MP, Callaghan TV, Carroll AB, Epstein HE, Jonsdottir IS, Klein JA, Magnusson B, Molau U, Oberbauer SF, Rewa SP, Robinson CH, Shaver GR, Suding KN, Thompson CC, Tolvanen A, Totland O, Turner PL, Tweedie CE. 2006. Plant community responses to experimental warming across the tundra biome. *Proceedings of the National Academy of Sciences of the United States of America* **103**: 1342–1346.

